Natural genetic variation underlying the negative effect of elevated CO_2 on ionome composition in *Arabidopsis thaliana*

Océane Cassan[1], Léa-Lou Pimparé[1], Timothy Mozzanino[1], Cécile Fizames[1], Sébastien Devidal[2], Fabrice Roux[3], Alexandru Milcu[2,4], Sophie Lèbre[5], Alain Gojon[1], Antoine Martin[1*]

[1] IPSiM, Univ Montpellier, CNRS, INRAE, Institut Agro, 34060, Montpellier, France

[2] Montpellier European Ecotron, Univ Montpellier, CNRS, Campus Baillarguet, 34980, Montferrier-sur-Lez, France

[3] Laboratoire des Interactions Plantes-Microbes-Environnement, Institut National de Recherche pour l'Agriculture, l'Alimentation et l'Environnement, CNRS, Université de Toulouse, Castanet-Tolosan, France

[4] CEFE, Univ Montpellier, CNRS, EPHE, IRD, UPVM, SupAgro, INRAE, 34293, Montpellier, France

[5] IMAG, Montpellier, France

*Author for correspondence: antoine.martin@cnrs.fr

Abstract

The elevation of atmospheric CO_2 leads to a decline in the plant mineral content, which poses a major threat to food security in the coming decades. To date, very few genes have been identified as having a role in the negative effect of elevated CO_2 on plant mineral composition. Yet, several studies have shown a certain degree of diversity in the ionome's response to elevated CO_2, associated with genotypic variation. This suggests the existence of genetic factors controlling the effect of CO_2 on ionome composition. However, no large-scale studies have been carried out to date to explore the genetic diversity of the ionome responses to elevated CO_2. Here, we used six hundred *Arabidopsis thaliana* accessions, representing geographical distributions ranging from worldwide to regional and local environments, to analyze the natural genetic variation underlying the negative effect of elevated CO_2 on the ionome composition in plants. We show that the growth under elevated CO_2 leads to a global and important decrease of the ionome content whatever the geographic distribution of the population. We also observed a high range of genetic diversity in the response of the ionome composition to elevated CO_2, and we identified sub-populations, showing effects on their ionome ranging from the most pronounced to resilience or even to a benefit in response to elevated CO_2. Using genome-wide association mapping on the response of each mineral element to elevated CO_2 or on integrative traits, we identified a large set of QTLs and genes associated with the ionome response to elevated CO_2. Finally, we demonstrate that manipulating the function of one of these genes can mitigate the negative effect of elevated CO_2 on the plant mineral composition. Therefore, this resource will contribute to understand the genetic mechanisms underlying the negative effect of elevated CO_2 on the mineral composition of plants, and to the development of biofortified crops adapted to a high-CO_2 world.

25 **Introduction**

26 The elevation of atmospheric CO_2 concentration leads to a decline in the mineral composition
27 of C3 plants [1]. The negative effect of elevated CO_2 on plant mineral composition has been
28 observed worldwide, and alters the content of nutrients that are essential for human
29 nutrition, such as nitrogen (N) and proteins, iron (Fe) or zinc (Zn) [2]. The rise in atmospheric
30 CO_2 thus poses a major threat to food security in the coming decades. The reasons why
31 elevated CO_2 leads to the degradation of plant mineral composition are far from being well
32 understood. To date, only a few genes with a potential regulatory effect on this mechanism
33 have been identified [3-7]. These elements nevertheless converge towards the fact that the
34 adaptation of plants to future high CO_2 climate can be achieved through the identification and
35 the characterization of genetic mechanisms. In addition to this, several studies suggest that
36 exploring the natural genetic variability of plants represents a major opportunity to
37 understand the mechanisms by which high CO_2 leads to a decline in plant mineral composition
38 [8-10]. Indeed, a significant diversity in the response of mineral composition to high CO_2 has been
39 observed in several plant species. For protein and therefore N content, as well as for Fe or Zn
40 content, substantial variations have been observed between small panels of genotypes from
41 different species [8-10]. This implies the presence of a genetic diversity reservoir, which can
42 facilitate the understanding of the ionome's response to high CO_2 and subsequently provide
43 an opportunity to alleviate this negative impact. However, in order to identify the genetic
44 determinants of this negative response of the ionome to high CO_2, large-scale approaches are
45 necessary, but are still lacking for the moment. The objective of this work was to fill the
46 aforementioned knowledge gap by using a large collection of natural genotypes of the model
47 plant *Arabidopsis thaliana* allowing to explore in depth the natural variation of the ionome
48 response to elevated CO_2, and to generate a resource of phenotypic data that can be used in

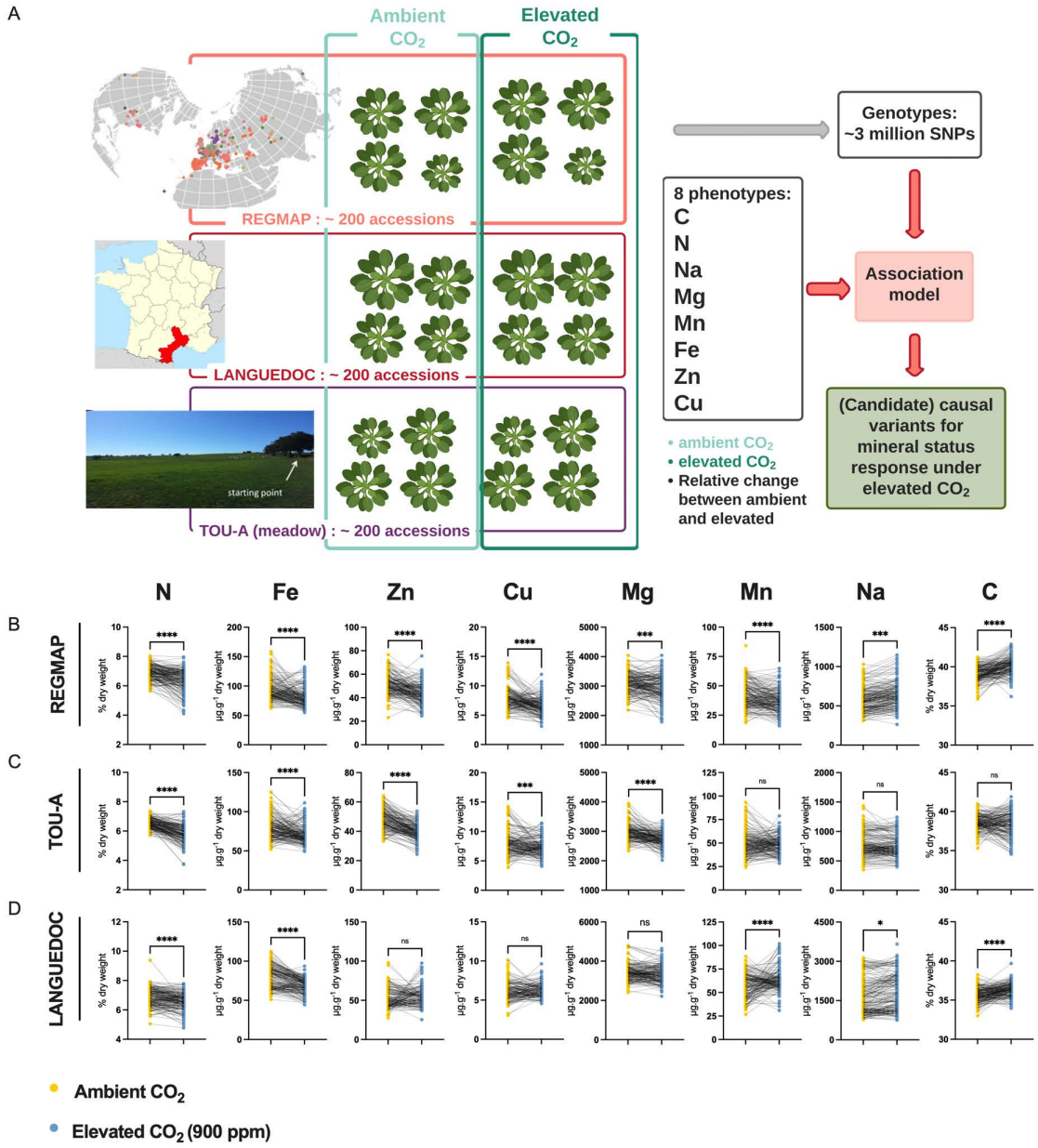

Figure 1: Elevated CO_2 negatively impacts the ionome content at the population-scale level in *Arabidopsis thaliana*. A. Representation of the experimental design used in this study. The content of eight mineral elements was assessed for around 600 *Arabidopsis thaliana* accessions coming from the REGMAP (B), LANGUEDOC (C) and TOU-A (D) populations. Each dot represents the value of the content of a mineral element for one accession (yellow: ambient CO_2 (aCO_2, ~420 ppm), blue: elevated CO_2 (eCO_2, 900 ppm). N (% of dry weight), Fe ($\mu g.g^{-1}$ dry weight), Zn ($\mu g.g^{-1}$ dry weight), Cu ($\mu g.g^{-1}$ dry weight), Mg ($\mu g.g^{-1}$ dry weight), Mn ($\mu g.g^{-1}$ dry weight), Na ($\mu g.g^{-1}$ dry weight), C (% of dry weight). Asterisks indicate significant differences (Paired Wilcoxson test; *, $P<0.05$; **, $P<0.005$; ***, $P<0.0005$). ns; not significant.

49 association genetics approaches. To this end, we used several hundreds of accessions from
50 different geographic scales of *A. thaliana*, and analyzed their mineral composition under
51 contrasted conditions of CO_2 concentration. This allowed us to extract the general trends in
52 the ionome response to high CO_2, and to identify a large set of genes associated with the
53 variation in the mineral composition of plants in response to high CO_2. By combining this
54 information with genome expression data under elevated CO_2, we end up by functionally
55 validating one of these genes for its importance in the reduction of Zn content under elevated
56 CO_2, and therefore by demonstrating the relevance of this resource for future improvement
57 of plant nutrient content under elevated CO_2.
58
59 **Results**
60 In order to explore the natural variation and identify its underlying genetic basis associated
61 with the negative effect of elevated CO_2 on plant ionome, we used three populations of *A.*
62 *thaliana* representing different geographic scales (i.e., the worldwide REGMAP population,
63 the LANGUEDOC regional population and the local TOU-A population from east of France) and
64 displaying different levels of genetic diversity (Fig. 1A). These populations were grown under
65 ambient or elevated CO_2, and we measured in each accession the composition of their ionome
66 in rosettes, including C, N, Na, Fe, Mg, Mn, Zn and Cu content.
67 **Elevated CO_2 globally decreases ionome content at the population level, whatever the**
68 **geographic scale.**
69 In the three *A. thaliana* populations, we observed a global and important decrease of the
70 ionome content when plants were grown under elevated CO_2 as compared to ambient CO_2.
71 This was particularly the case for N and Fe, for which the decrease in content was very robust
72 and important in each of the population analyzed (Fig. 1B-D). Zn, Cu and Mg content were also

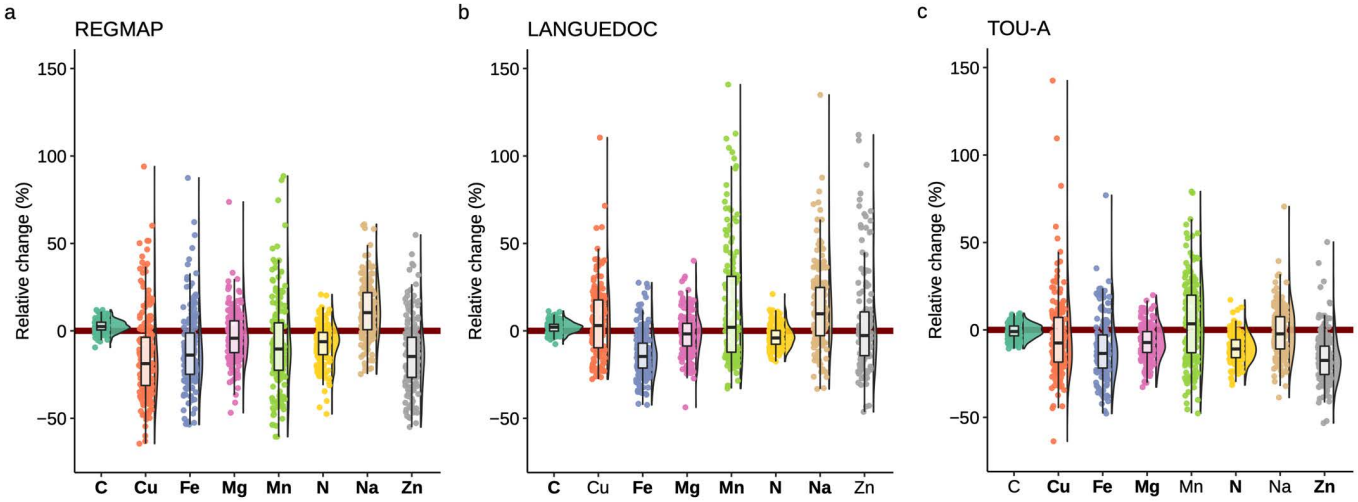

Figure 2: Elevated CO_2 leads to high phenotypic diversity of ionome response in *Arabidopsis thaliana*. Distributions of the relative change (%) of the content of 8 mineral elements between elevated CO_2 and ambient CO_2, in each population (A: REGMAP, B: LANGUEDOC, C: TOU-A). Each dot represents the value of the relative change of the content a mineral element for one accession. The name of the element appears in bold if the mean of the element in elevated CO_2 is significantly different from the mean of the element in ambient CO_2 (Paired wilcoxon test, significance threshold of 0.05).

73 negatively affected to a significant extent by the growth under elevated CO_2 in the REGMAP
74 and in the TOU-A populations (Fig. 1B, C), although not significantly in the LANGUEDOC
75 population (Fig. 1D). More variability for the effect of elevated CO_2 was observed on Mn and
76 Na content, which were decreased in the REGMAP population, but not significantly changed
77 in the TOU-A and LANGUEDOC populations, respectively. In parallel, the C content of these
78 populations increased under elevated CO_2, by very significant factors for the REGMAP and the
79 LANGUEDOC populations. Altogether, these observations demonstrate that elevated CO_2 has
80 on average a strong negative impact on the mineral content of natural genotypes of *A.*
81 *thaliana* at the population-scale, whatever their geographic distribution.
82
83 **The ionome of *Arabidopsis thaliana* natural accessions displays a high range of phenotypic**
84 **diversity in response to elevated CO_2.**
85 To explore the effect of elevated CO_2 in each accession, we calculated the relative change in
86 nutrient composition of *A. thaliana* accessions from the three populations in response to
87 elevated CO_2. In agreement with the results previously mentioned, we observed that the
88 median relative change of most nutrient content at the population-level was negatively
89 affected by elevated CO_2 (Fig. 2). But the most striking observation was the genetic diversity
90 of ionome response observed in these populations. Indeed, while most the natural accessions
91 were negatively affected by elevated CO_2 (with a negative relative ratio of their nutrient
92 content between ambient and elevated CO_2), a considerable number of accessions were
93 rather not affected by elevated CO_2, or even positively affected, therefore showing an
94 improved nutrient composition under elevated CO_2. For macronutrients like N, the relative
95 change of concentration between ambient and elevated CO_2 varied from 20% to -50%, and for
96 micronutrients like Cu, Fe or Zn, the relative change of concentration between ambient and

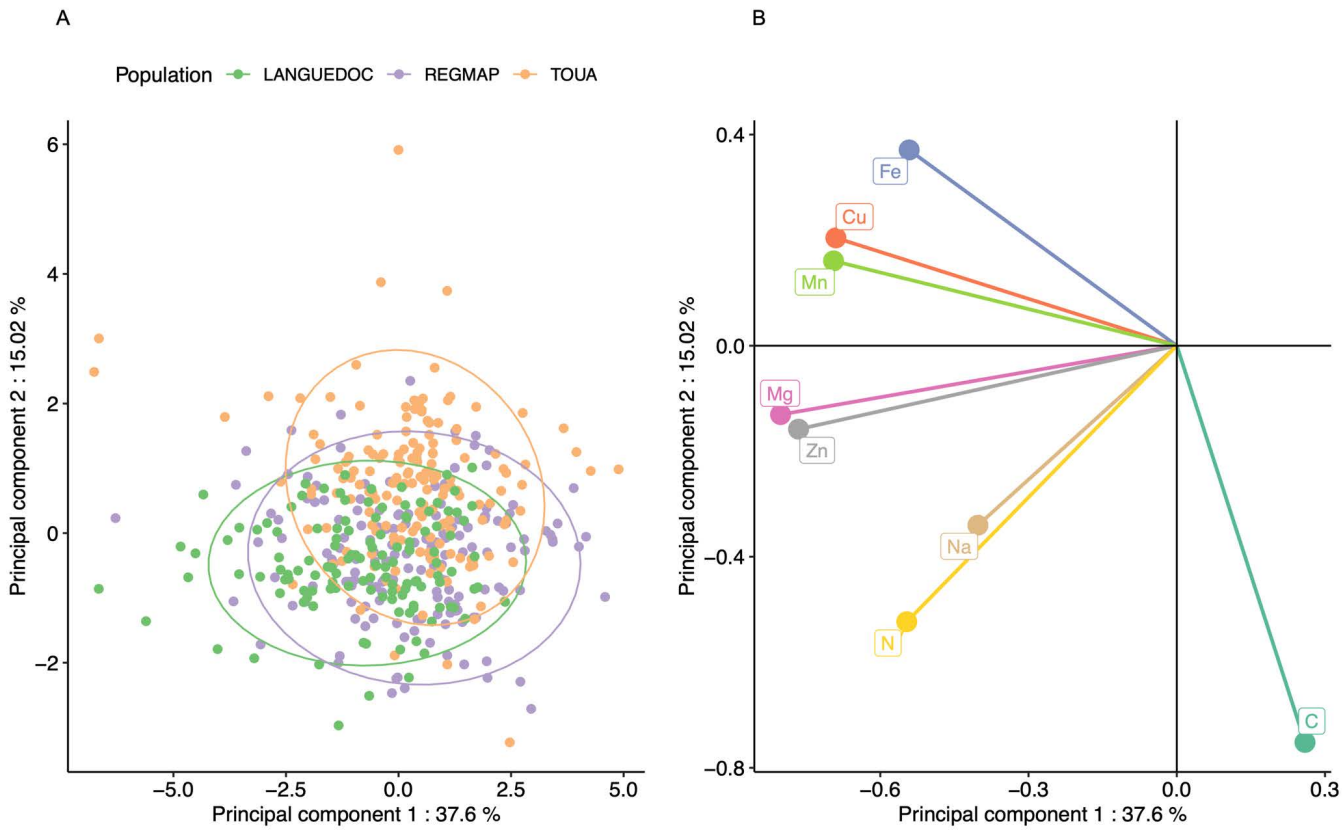

Figure 3: Elevated CO_2 results in a general pattern of ionome variation common to most accessions constituting natural populations of *Arabidopsis thaliana.* Principal Component Analysis (PCA) was performed using the variation of each element in response to elevated CO_2. A. Natural accessions were positioned on the PCA and colored based on population. B. Contribution of each element to the PCA axis.

97 elevated CO_2 varied from 100% to -60% (Fig. 2). In addition, some differences among nutrients
98 were observed between populations. For instance, a smaller dispersion of Fe relative change
99 in the LANGUEDOC population, against a higher distribution of Mn relative change.
100 In order to explore the behavior of the different elements in response to elevated CO_2 and to
101 observe the structure of phenotypic variation, we performed a principal component analysis
102 (PCA) of the relative change in the 8 elements for the accessions from the three populations.
103 The accessions from all populations seem to have globally similar responses to elevated CO_2,
104 as suggested by the overlap of the three populations in the two first principal components
105 (Fig. 3A). The first component of the PCA described a clear antagonistic trend between C
106 content and the change of other mineral elements (Fig. 3B), suggesting that most of the
107 variation between accessions in term of mineral response (almost 40%) could be driven by
108 one or a few mechanisms resulting in an inverse variation between the whole ionome and C
109 change (Fig. 3B). Interestingly, the second component, explaining almost 15% of the variation
110 among accessions in term of mineral response, was mainly driven jointly by change in N and
111 C concentration. Altogether, these results show that there is a marked and large variability
112 among accessions in their mineral concentration in response to elevated CO_2, illustrated by
113 accessions negatively affected by elevated CO_2 and others positively affected by elevated CO_2.
114 In order to explore specific behavior of sub-populations, we clustered the accessions from the
115 REGMAP panel via a k-means approach. This multivariate clustering resulted in the
116 partitioning of accessions in three groups (Fig.4 – Suppl. Table 1). Cluster 1 displayed the most
117 negative pattern of ionome response to elevated CO_2. Inversely, accessions included in Cluster
118 2 displayed a globally positive response, with the highest relative change for almost all mineral
119 elements, except for C content. These accessions did not appear to be clustered
120 geographically with respect to their collection origin in the REGMAP panel (Suppl. Fig. 1),

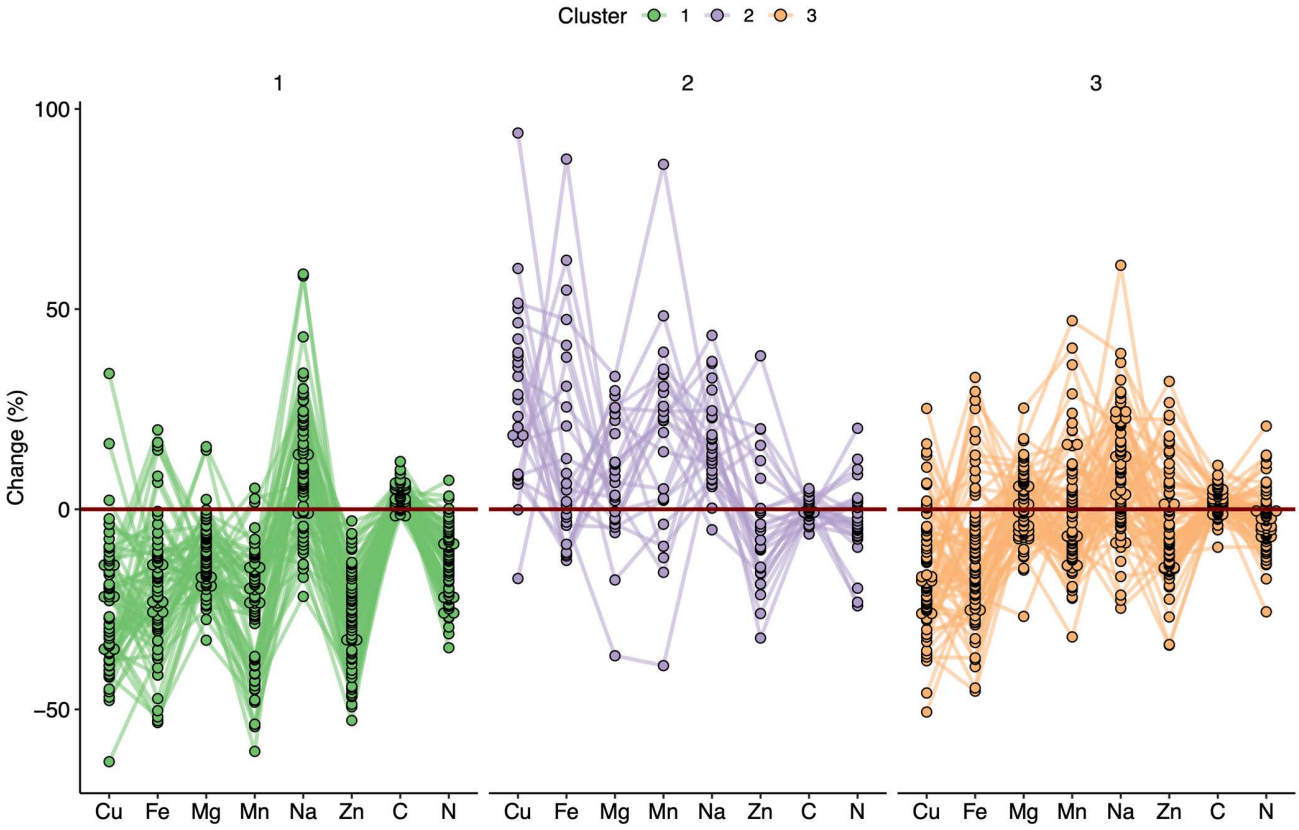

Figure 4: Variation in the response of the ionome to elevated CO_2 identifies contrasting subpopulations inside the REGMAP panel. K-means clustering was performed in the REGMAP accessions to identify different subpopulations. Each accession is represented by a dot, connected by a line between each element. Cluster 1:65 accessions. Cluster 2: 25 accessions. Cluster 3: 69 accessions.

121 which is in line with the high genetic diversity of response to elevated CO_2 observed at smaller
122 geographical scales (Fig.2). Finally, Cluster 3 displayed a resilient pattern, with accessions
123 showing a globally attenuated response to elevated CO_2. Interestingly, the large phenotypic
124 diversity of the ionome observed in the three populations in response to high CO_2, as well as
125 the presence of contrasted subpopulations in the REGMPA panel, suggests the presence of
126 genetic determinants associated with this response.
127
128 **Genetic architecture of the ionome response to elevated CO_2, and identification of genetic**
129 **determinants**
130 We run Genome-Wide Association (GWA) mapping to describe the genetic architecture of the
131 ionome response to elevated CO_2, and to fine-map candidate genes underlying the detected
132 quantitative trait loci (QTLs). We focused here on the phenotypic data collected on the
133 REGMAP population, and used the sequencing data available for this population [11]. We
134 included in this analysis the level of each mineral under ambient and under elevated CO_2, as
135 well as the relative change between ambient and elevated CO_2 for each element. We also
136 included a trait corresponding for each accession to the coordinate on the first and on the
137 second PCA axes (PCA1 and PCA2) explaining collectively more than 50% of ionomic variation
138 (Fig. 3). Therefore, these values correspond to traits driving and summarizing a large part of
139 the ionome variation under elevated CO_2. This resulted as a whole in running GWA mapping
140 on 30 different single-trait GWAS. The overall approach was first validated by observing
141 expected results for traits phenotyped under ambient CO_2. For instance, we observed a very
142 strong peak for the Na content at the locus of the *HKT1* gene (Suppl. Fig. 2A), which is known
143 to be involved in the natural genetic variation of Na content in *Arabidopsis thaliana* [12], or a
144 strong peak for the N content at the locus of the *NIA1* gene (Suppl. Fig. 2B), encoding for an

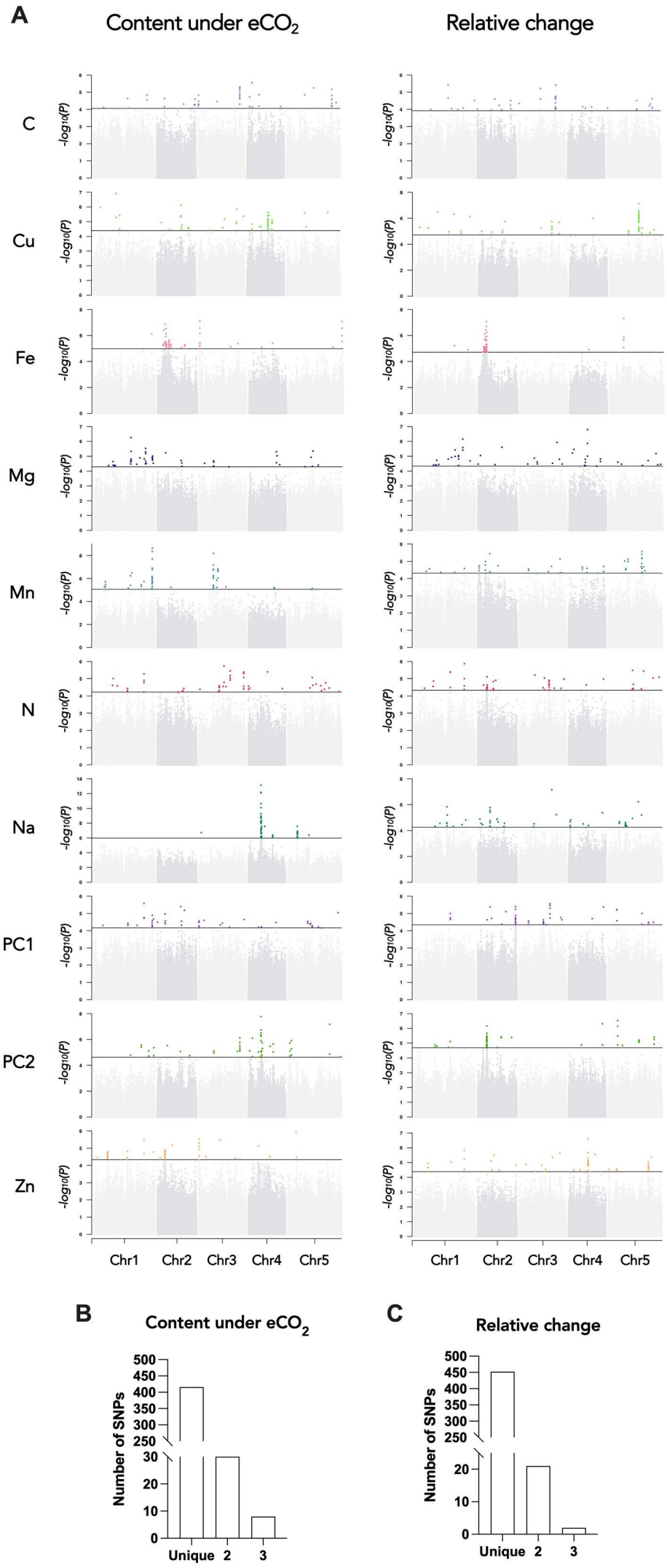
A
Content under eCO2
Relative change
C
Cu
Fe
Mg
Mn
N
Na
PC1
PC2
Zn
-log10(P)
Chr1
Chr2
Chr3
Chr4
Chr5
B
Content under eCO2
Number of SNPs
Unique
2
3
C
Relative change
Number of SNPs
Unique
2
3

Figure 5: Genetic architecture of the response of the ionome to elevated CO_2 in the REGMAP panel of *Arabidopsis thaliana*. A. Manhattan plots for the content of eight mineral elements under elevated CO_2, or for the relative change of the content of mineral elements between elevated CO_2 and ambient CO_2. For each Manhattan plot, SNPs with the 50 most significant P-value, located above the horizontal line, are colored. Bar plots showing the number of SNPs identified by GWAs for traits under elevated CO_2 (B) or for the relative change of the content of mineral elements between elevated CO_2 and ambient CO_2 (C) that are unique to one element or shared between 2 or 3 traits.

145 isoform of the nitrate reductase required for the first step of nitrate reduction and associated
146 with natural genetic variation of N content in *A. thaliana* [13].
147 GWA mapping revealed a polygenic architecture for each phenotypic trait, although its
148 complexity largely differs among traits. For instance, very few and neat peaks of association
149 were detected Na and Mn content under elevated CO2, or of Fe and Cu relative change
150 between ambient and elevated CO2 (Fig.5A, Suppl. Fig. 3). On the other hand, a more complex
151 genetic architecture with the detection of a large number of QTLs was observed for traits
152 related to N or C content (Fig.5A, Suppl. Fig. 3). For each of the traits that have been analyzed
153 under elevated CO_2 or corresponding to the relative change of their content between ambient
154 and elevated CO_2, we isolated the 50 SNPs with the most significant p-value, hereafter named
155 top SNPs (Fig. 5A, Suppl. Tables 2 and 3). In order to identify the overlap between the genetic
156 architecture of each trait, we looked whether some of the top SNPs were shared among traits.
157 While the large majority of SNPs were specific to one trait, 30 and 21 SNPs were shared
158 between two traits for the content under elevated CO_2 or for the relative change between
159 ambient and elevated CO_2, respectively (Fig. 5B and C, Supplemental Tables 2 and 3). In
160 addition, 8 and 2 SNPs were shared between three traits for the content under elevated CO_2
161 or for the relative change between ambient and elevated CO_2, respectively (Fig. 5B and C,
162 Supplemental Tables 2 and 3). Most of the shared SNPs were associated with micronutrients
163 (Fe, Mn, Zn and Mg content) and with N and/or with the first component of the PCA axis. An
164 interesting QTL located on chromosome 1 was notably associated with 6 traits, displaying
165 SNPs shared between Mn, Zn and N relative change and SNPs shared between Mn, N and PC1
166 content under elevated CO_2 (Fig. 5A, Suppl. Tables 2 and 3). Another QTL located on
167 chromosome 3 encompasses SNPs shared between Fe, Zn and PC1 content under elevated
168 CO_2 (Fig. 5A, Suppl. Table 2).

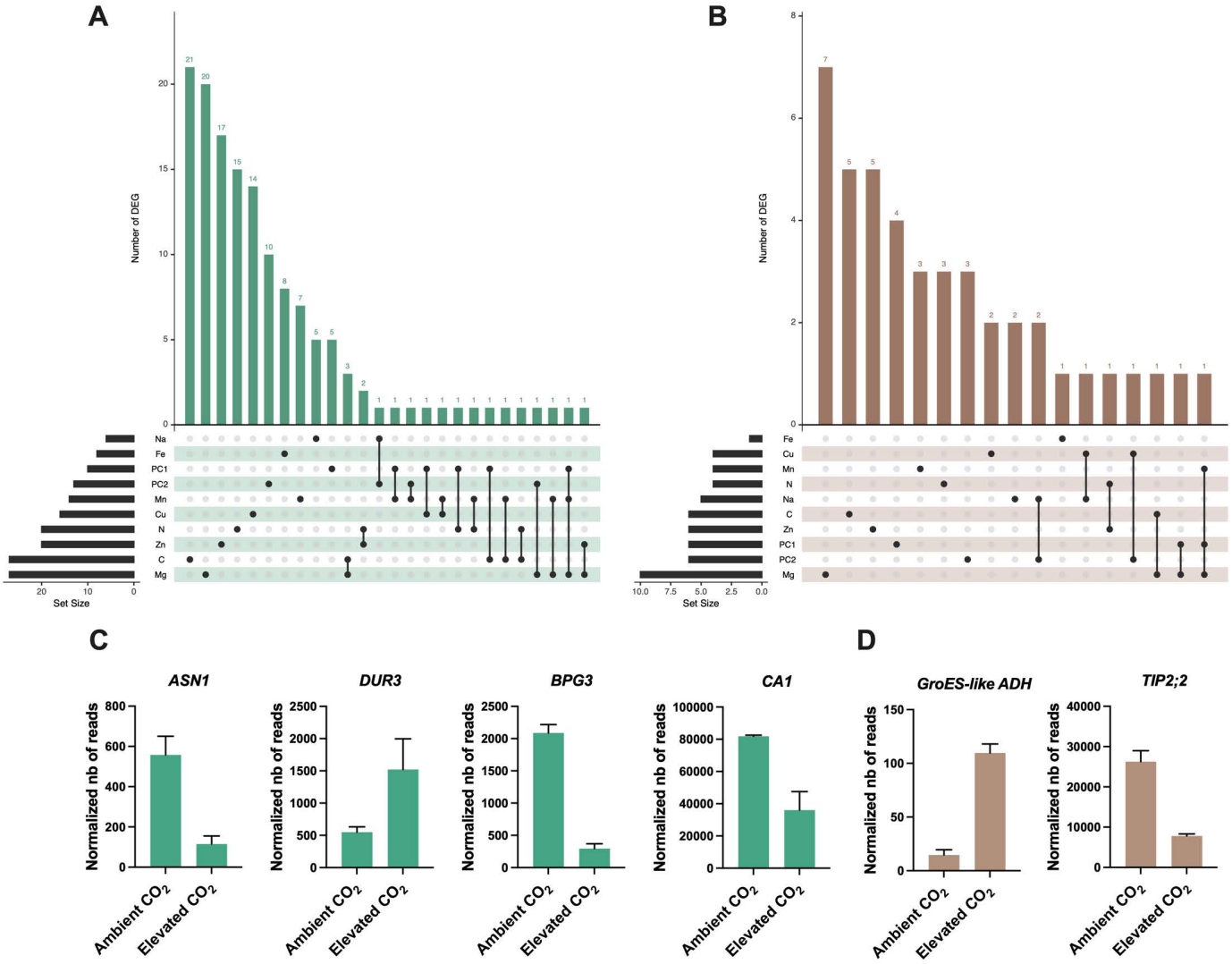

Figure 6: Identification of genes detected by GWA mapping and differentially regulated by elevated CO_2. Intersection between elevated CO_2-DEG in shoot (A) or root (B) and genes identified by GWA mapping. UpSet plots display the number of elevated CO_2-DEG that are associated to a locus identified for the content or the relative change of one or several mineral elements under elevated CO_2. Illustration of the pattern of elevated CO_2-DEG in shoot (C) or root (D) also identified by GWA mapping.

169 We next identified for each trait a list of the genes located at ±25 kb from the top 50 SNPs,
170 which corresponds to the rough estimate of the decay of linkage disequilibrium identified in
171 *A. thaliana* at the worldwide scale [14]. This resulted in a list of genes for each element, ranging
172 from 154 to 422 genes depending on the element (Suppl. Tables 2 and 3). Among others,
173 several genes associated with top 50 SNPs were identified as obvious candidates of the effect
174 of elevated CO_2 on plant nutrition and ionome content. This was the case of *ZINC INDUCED*
175 *FACILITATOR 1* (*ZIF1*, *AT5G13740*) and *ZIF-LIKE1* (*AT5G13750*), linked with SNPs identified for
176 Zn content under elevated CO_2, and involved Zn sequestration mechanisms [15]. We also noticed
177 the link between SNPs identified for Zn relative change and *TIP2;2* (*AT4G17340*), known to be
178 involved in Zn root-to-shoot translocation [16]. Concerning N relative change, some of the top
179 50 SNPs were linked to *ASN1* (*AT3G47340*), which is an actor of N status and remobilization
180 [17,18]. The *H+/CATION EXCHANGER 1* (*CAX1*) gene (*AT2G38170*), involved in the response to Mn
181 deficiency, was also linked to SNPs associated with Mn content under elevated CO_2 [19]. Some
182 of the top 50 SNPs identified for Fe relative change were linked to *MCO2* (*AT5G21100*) and
183 *MCO3* (*AT5G21105*) genes, which have been recently characterized as actors of the regulation
184 of Fe homeostasis [20]. Finally, it is interesting to note that the QTL located on chromosome 3
185 mentioned above displaying significant shared SNPs identified for Fe, Zn and PC1 content
186 under elevated CO_2 was associated among other genes with *ISU2* (*AT3G01020*), coding for one
187 of the Fe-S clusters in *Arabidopsis thaliana*, which are known to be essential for
188 photosynthesis and metabolism [21]. Altogether, this demonstrated that genes identified
189 through this approach represent a large and valuable reservoir of candidates to study and to
190 counteract the effect of elevated CO_2 on plant nutrition and ionome content.
191 To analyze how these genes identified by GWA mapping are regulated by elevated CO_2, we
192 performed RNA-seq from shoots and roots grown under ambient and elevated CO_2.

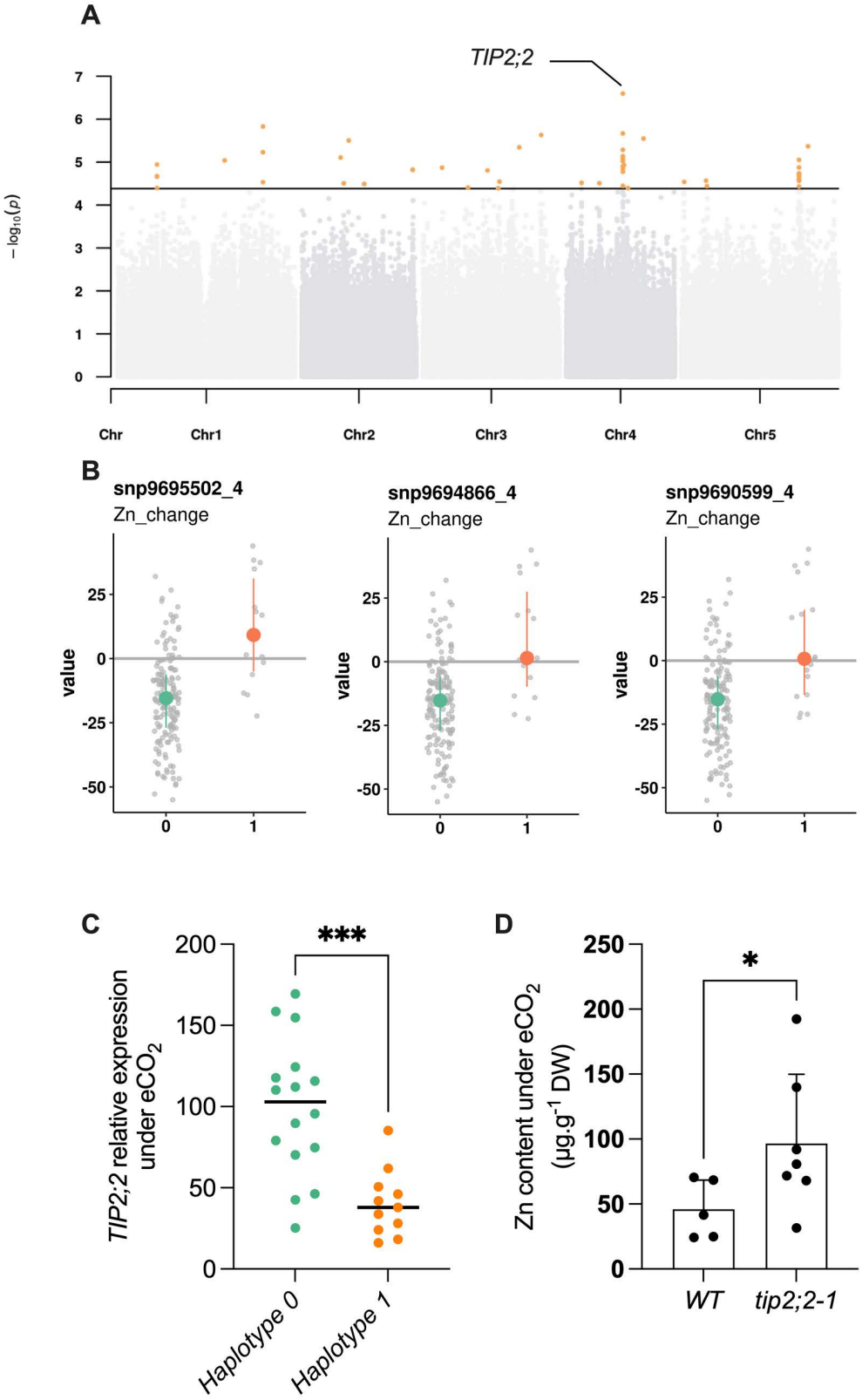

Figure 7: Natural variation of the *TIP2;2* gene is associated with improved responses of Zn content to elevated CO_2. Manhattan plot of the relative change of Zn content between elevated CO2 and ambient CO2 showing the presence of a peak closed to the *TIP2;2* locus. B. Comparison of haplotypes and their relative change of Zn content between elevated CO_2 and ambient CO_2. Three SNPs located at the *TIP2;2* locus are associated to an improvement of Zn content under elevated CO_2 for accessions that possess them (haplotype 1) compared to the rest of the population (haplotype 0). C. Relative expression of *TIP2;2* in the roots under elevated CO_2 for accessions belonging to haplotype 0 or haplotype 1. Relative expression levels were calculated based on *UBQ10* as internal control. Horizontal black line represented the median of each group of haplotypes. ***P < 0,001, unpaired Mann-Whitney test. D. Shoot Zn content under elevated CO_2 for WT (Columbia) and *tip2;2-1* mutant belonging to haplotype 0 or haplotype 1. Data are presented as the mean (with SD) of 5 and 6 biological repeats for the WT and *tip2;2-1*, respectively. *P < 0.05, unpaired Mann-Whitney test.

193 Differentially expressed genes (DEG) associated to the effect of elevated CO_2 were identified
194 from shoots and roots (Suppl. Table 4). We crossed the list of shoots or roots elevated CO_2-
195 DEG with the list of genes identified by GWA mapping for each element, which resulted in a
196 list of 182 genes identified by GWA mapping and differentially regulated by elevated CO_2 in
197 shoot or in roots (Suppl. Table 5), making them strong candidates to be involved in the
198 response of the mineral composition of plants to elevated CO_2. Most of these genes were
199 deregulated by elevated CO_2 in shoot (Fig. 6A, B). In shoot or in roots, these genes mainly
200 showed an association with C-, Mg- or Zn-related traits (Fig. 6A, B). Several of these genes,
201 identified by GWA mapping and whose expression is deregulated in response to high CO_2,
202 were known for their role in nutrient homeostasis. This was the case for the *ASN1* and *DUR3*
203 genes, encoding an asparagine synthase and a urea transporter involved in N metabolism and
204 remobilization, both associated here with a N-related peak of association, and whose
205 expression is modulated by high CO_2 in leaves (Fig. 6C). We also observed in the leaves an
206 interesting profile for several genes related to C metabolism and photosynthesis. This was the
207 case for the *BGP3* gene, involved in chloroplast development, or for the carbonic anhydrase
208 *CA1*, both showing a decreased expression in response to high CO_2 and both associated with
209 a peak in C-related GWA mapping under elevated CO_2 (Fig. 6C). In roots, the gene most
210 deregulated in response to high CO_2 was *AT1G64710*, encoding a GroES-type alcohol
211 dehydrogenase, which interestingly is also deregulated in leaves (Fig. 6D). We also observed
212 in the roots that the expression of the *TIP2;2* gene, associated here with a peak detected for
213 Zn relative change GWA mapping, was deregulated in response to elevated CO_2 (Fig. 6D).
214 To go further, we selected one of the association peaks identified by GWA mapping, and
215 sought to functionally validate the importance of this QTL in response to elevated CO_2, in order
216 to demonstrate the value of our data set and GWA mapping analyses. To do so, we selected

217 an association peak located on chromosome 4 and associated with Zn relative change (Fig.
218 7A). More precisely, this association peak displayed the SNPs with the most significant *p*-
219 values and more largely three SNPs that fell into the top 10 SNPs of the trait corresponding to
220 the Zn relative change between ambient and elevated CO_2. The SNPs corresponding to the
221 alternative alleles were associated to an increase of Zn content under elevated CO_2 (Fig. 7B).
222 These SNPs are located very close to the *TIP2;2* (*AT4G17340*) gene, which has been recently
223 characterized as an actor of Zn root-to-shoot translocation [16]. We thus selected a set of
224 accessions from haplotype 0 (reduced Zn content under elevated CO_2) or haplotype 1
225 (increased Zn content under elevated CO_2), and analyze *TIP2;2* expression in the roots under
226 elevated CO_2. This analysis revealed a haplotype-specific difference in *TIP2;2* expression under
227 elevated CO_2, with accessions from haplotype 1 showing a reduced *TIP2;2* expression in the
228 roots compared to those from haplotype 1 (Fig. 7C), correlated with a higher Zn content in the
229 shoot (Fig. 7B). To validate the effect of *TIP2;2* expression of Zn content under elevated CO_2,
230 we used the *tip2;2-1* knock-out mutant and compared its Zn content under elevated CO_2 to
231 this of the WT. We observed that the *tip2;2-1* mutant line displayed a significant higher Zn
232 content in the shoot under elevated CO_2 compared to the WT, confirming that *TIP2;2*
233 expression determines Zn content under elevated CO_2 (Fig. 7D). Altogether, these results
234 demonstrated that these data sets generated in this study and the associated analyses are a
235 valuable resource to identify genes able to counteract the general negative effect of elevated
236 CO_2 on the mineral composition of plants.
237

238 **Discussion**

239 **The natural variation of ionome response to elevated CO_2 in *Arabidopsis thaliana* displays a**
240 **high degree of genetic variation**

241 In the present work, we analyzed the diversity of ionome response to elevated CO_2 present in
242 the natural variation of *Arabidopsis thaliana*. In agreement with several other phenotypic
243 traits related to phenology and disease resistance {Brachi, 2013 #1232;Huard-Chauveau, 2013
244 #1247;Roux, 2022 #1248}, we observed a wide range of responses at complementary
245 geographical scales, from accessions with a ionome strongly negatively affected by high CO_2
246 to accessions with a ionome benefiting from high CO_2. This confirms for the first time on large
247 and complementary sets of natural genotypes what has been observed by meta-analysis on
248 isolated groups of plants worldwide [2,9]. The global analysis of the distribution of each mineral
249 element studied suggests firstly a trend where the whole ionome would evolve in a unified
250 manner in response to high CO_2, and in an opposite manner to C. This is in line with a number
251 of studies that have proposed that the accumulation of carbohydrates due to the stimulation
252 of photosynthesis by high CO_2 would be the cause of the decrease in plant mineral
253 composition [22-25]. However, the reading of the genetic architecture performed here by a
254 genome-wide association genetics approach suggests that the majority of the genetic
255 mechanisms underlying the negative effect of elevated CO_2 on the ionome are specific to each
256 mineral element. Some specific cases, such as the QTL detected on chromosome 1 and
257 associated with the natural genetic variation of 6 traits among the 20 considered, will certainly
258 deserve a more in-depth analysis.
259 By clustering globally distributed accessions according to their ionome sensitivity to high CO_2,
260 we were able to observe that the geographic origin of the accessions likely did not determine
261 their response to CO_2. This suggests that inherent genetic factors, more than those due to
262 local adaption, direct the response of plants to elevated CO_2. This seems consistent since the
263 CO_2 elevation applied here to natural *Arabidopsis thaliana* variants does not correspond to
264 any environment experienced by plants yet, at least for several tens of millions of years [26,27].

265 In this context of brutal and highly impactful environmental change, the presence of cryptic
266 genetic variation often explains the appearance of relatively rapid adaptive mechanisms [28,29].
267 Although not formally tested here, it would be interesting to examine whether the variation
268 in the ionome in response to elevated CO_2 shows evidence of cryptic variation. In any case,
269 the presence of high phenotypic diversity in these natural populations of *A. thaliana*
270 demonstrates very clearly the possibility of taking advantage of this genetic variation to
271 understand and alleviate the negative response of plant mineral composition to high CO_2.

272 **GWA mapping of ionome variation under elevated CO_2 identified a large number of genes**
273 **to understand and mitigate the negative effect of high CO_2 on plant mineral composition**

274 In order to understand the genetic mechanisms underlying the effect of high CO_2 on plant
275 mineral composition, and to enable future breeding approaches, we adopted an association
276 genetics approach. This led to the identification of a large number of candidate genes
277 associated to the variation of nutrients under elevated CO_2. Several genes in this list can easily
278 attract attention. In particular, we can note the identification of *ASN1* and *DUR3* genes in two
279 of the loci associated with N content variation under elevated CO_2. *ASN1*, and to a lesser
280 extent *DUR3*, play an important role in the remobilization and the reallocation of N within the
281 plant, and their manipulation can lead to variation in N use efficiency [17,18,30]. This is interesting
282 because for the moment, root N uptake and N assimilation seemed to be the key targets of
283 the negative effect of high CO_2 on plant N content [4,31], but these results suggest that
284 remobilization of N may also be involved. We also identified the *CA1* gene, coding for a
285 carbonic anhydrase, in the vicinity of a QTL associated with C variation under high CO_2. *CA1* is
286 involved in the regulation of stomatal opening by elevated CO_2 [32], and the β carbonic
287 anhydrase family of which *CA1* belongs is involved in the regulation of photosynthetic
288 efficiency, although *CA1* shows no significant effect under standard conditions [33]. It would be

289 therefore interesting to assess the role of *CA1* natural genetic variation under elevated CO_2. If
290 *CA1* regulates the C variation of the ionome under elevated CO_2, this could, according to our
291 observations, significantly influence the global mineral composition of plants. Interestingly,
292 the genes identified by GWA mapping in the ionome response to high CO_2, including those
293 mentioned above, showed substantial variation at the gene expression level. We ended this
294 study with the functional validation of an association peak identified by GWA mapping for the
295 relative change of Zn content between ambient and elevated CO_2. Zn is an essential element
296 for a large number of metabolic processes in humans, and Zn deficiency, found in up to one
297 third of the world's population, leads to severe health problems. We demonstrated that *TIP2;2*
298 gene expression varied in response to CO_2 in a haplotype-specific manner. Consistent with
299 these results, we show that manipulating *TIP2;2* expression with a knock-out mutant can
300 modulate the Zn loss observed under high CO_2. A recent study demonstrated that TIP2;2 was
301 responsible for Zn retention in the roots {Wang, 2022 #1177}. It therefore seems consistent
302 that natural accessions with the lowest expression levels of this gene are those with the
303 highest Zn content in aerial parts, due to low retention in their roots. This example illustrates
304 the potential of the resource we have generated here towards the development of biofortified
305 plants. The development of biofortified plants represents a considerable challenge in view of
306 the current problems of malnutrition on a global scale, and this challenge becomes even more
307 important in a context of rising atmospheric CO_2 [34]. This reservoir of data and genes will
308 certainly contribute to the understanding of the mechanisms underlying the general negative
309 effect of CO_2 on mineral composition, and to the development of crop plants adapted to
310 forthcoming high-CO_2 climate.
311
312 **Methods**

313 *Data and code availability*

314 Data and R notebooks containing the analyses performed in this article can be found at

315 https://src.koda.cnrs.fr/groups/ipsim/sirene-team. RNA-seq data generated for this study are

316 available at https://www.ebi.ac.uk/biostudies/arrayexpress/studies using the accession no

317 xxx.

318 *Plant Material*

319 A subset of the REGMAP panel, the LANGUEDOC panel and the TOU-A panel were used in this

320 study. These populations were previously described here {Brachi, 2013 #1232;Frachon, 2017

321 #1249;Horton, 2012 #1231}. These populations were grown on Jiffy-7 peat pellets (Jiffy

322 Products International, NL) under ambient (~420 ppm) or elevated (900 ppm) CO_2 in the

323 growth chambers of the Microcosms experimental platform at the Montpellier European

324 Ecotron CNRS. Growth conditions were 6-h/22-h light (22°C) / dark (20°) photoperiod, with

325 200 µmol m^{-2} s^{-1} light intensity and 65% of hygrometry. Plants were watered twice a week

326 with a growth solution containing KH_2PO_4 1 mM, $MgSO_4$ 1 mM, K_2SO_4 250 µM, $CaCl_2$ 250 µM,

327 Na-Fe-EDTA 100 µM, KNO_3 10 mM, KCl 50 µM, H_3BO_3 30 µM, $MnSO_4$ 5 µM, $ZnSO_4$ 1 µM, $CuSO_4$

328 1 µM, $(NH_4)_6Mo_70_{24}$ 0,1 µM, as described by [35]. The entire rosettes were collected three weeks

329 after sowing. The *tip2;2-1* mutant line corresponds to the *SALK_152463* allele [16].

330 *Ionome analysis*

331 From 3 to 5 replicates per accession were used for each ionome analysis. Total C and N content

332 was obtained from dried shoot tissue using an Elementar Pyrocube analyzer. Cu, Fe, Mg, Mn,

333 Na and Zn content was obtained from dry shoot tissue mixed with 750 µl of nitric acid (65%

334 [v/v]) and 250 µl of hydrogen peroxide (30% [v/v]). After one night at room temperature,

335 samples were mineralized at 85°C during 24 hours. Once mineralized, 4 ml of milliQ water was

336 added to each sample. Mineral contents present in the samples were then measured by
337 microwave plasma atomic emission spectroscopy (MP-AES, Agilent Technologies).

338 *Removal of outlier observations*

339 Prior to GWAS and multivariate analyses such as PCA or clustering, mineral composition
340 measures were pre-processed to remove technical outliers. For a given element and CO_2
341 condition, the values positioned more than 5 median absolute deviations away from the
342 median were removed from the dataset.

343 *PCA and Clustering*

344 Principal Component Analysis was performed using the R *ade4* package after the prior scaling
345 of the variables to a z-score. Clustering of the REGMAP panel based on the relative changes of
346 the mineral composition of each accession has been done using a k-means clustering with the
347 R *kmeans* function. For this step, the variables were also scaled to a z-score. The number of
348 clusters in the k-means algorithm was chosen by the elbow method on the criteria of cluster
349 homogeneity (within-sum of squares).

350 *GWAs*

351 Genome-Wide Association mapping was performed using the R *statgenGWAs* package.
352 Genotype data was prepared using the *codeMarkers* function, removing duplicated SNPs and
353 filtering for a minimum allele relative frequency of 0.04. Associations were performed by the
354 *runSingleTraitGwas* function, that implements the EMMA algorithm. Population structure was
355 modeled via a kinship matrix built from the Astle method. Manhattan plots were drawn using
356 the *manPlotFast* function of the *ramwas* R package.

357 *RNA-seq experiments*

358 Plants were grown in hydroponics to have access to the roots in addition to the shoot, as
359 previously described in [4]. Shoot or root from 5 plants were pooled into one biological replicate,

360 flash frozen in liquid nitrogen, and stored at -80◦C. RNA of three biological replicates were
361 extracted from shoot or root tissues using Direct-zol RNA Miniprep (Zymo Research, CA, USA),
362 according to the manufacturer recommendations. RNA-sequencing libraries were done from
363 shoot or root total RNA using standard RNA-Seq protocol method (Poly-A selection for mRNA
364 species) by the Novogene company. RNA-sequencing was performed using Illumina
365 technology on a NovaSeq6000 system providing PE150 reads. The quality control and adapter
366 trimming of raw paired-end fastq files was done with *fastp* and its default parameters.
367 Mapping to the TAIR10 reference genome was performed with STAR, and using the following
368 options:
369 --outSAMtype BAM SortedByCoordinate
370 --outFilterMismatchNmax 1
371 --outFilterMismatchNoverLmax 0.15
372 --alignIntronMin 30
373 --alignIntronMax 5000
374 Quantification of the bam files against the TAIR10 GFF3 annotation file was done using *htseq-*
375 count with options:
376 -f bam --type gene -r pos
377 --idattr=Name --stranded=no
378 Normalization and differential expression were performed using *DIANE* R package [36], with no
379 fold change constraint, and an adjusted p-value threshold (FDR) of 0.05. Lowly expressed
380 genes with an average value across conditions under 25 reads were excluded from the
381 analysis.
382 *Quantitative real-time PCR*

383 Plants were grown in hydroponics to have access to the roots, as previously described in [4].
384 Root tissue from 5 plants were pooled into one biological replicate, flash frozen in liquid
385 nitrogen, and stored at -80◦C. RNA were extracted from shoot or root tissues using TRIZOL
386 (Invitrogen, USA), according to the manufacturer recommendations, and DNAse treated using
387 RQ1 (Promega, USA). Reverse transcription was achieved from 1 μg of total RNA with M-MLV
388 reverse transcriptase (RNase H minus, Point Mutant, Promega, USA) using an anchored
389 oligo(dT)20 primer. Accumulation of transcripts was measured by qRT-PCR (LightCycler 480,
390 Roche Diagnostics, USA) using the SYBR Premix Ex TaqTM (TaKaRa, Japan). Gene expression
391 was normalized using *UBQ10* and *ACT2* as internal standards. Results are presented as the
392 expression relative to *UBQ10*. Sequences of primers used in RT-qPCR for gene expression
393 analysis are listed in Supplemental Table 6.
394
395 **Acknowledgments**
396 This work was supported by the I-Site Montpellier Université d'Excellence (MUSE; project
397 ECO2THREATS), the CNRS through the Mission for Transversal and Interdisciplinary Initiatives
398 (MITI) 80 PRIME program, and the Plant Biology and Breeding department of INRAE. O.C. was
399 recipient of a PhD fellowship from the CNRS. T.M. was recipient of a PhD fellowship from
400 INRAE and Région Occitanie. We thank Jiping Liu from Cornell University for the gift of *tip2;2-*
401 *1* mutant line. This study benefited from the CNRS human and technical resources allocated
402 to the Ecotron Research Infrastructure and from the state allocation "Investissement
403 d'Avenir" AnaEE France ANR-11-INBS-0001. A CC-BY public copyright license has been applied
404 by the authors to the present document.
405

406 **References**

407 1 Gojon, A., Cassan, O., Bach, L., Lejay, L. & Martin, A. The decline of plant mineral
408 nutrition under rising CO2: physiological and molecular aspects of a bad deal. *Trends*
409 *in Plant Science* **28**, 185-198 (2023). https://doi.org:10.1016/j.tplants.2022.09.002

410 2 Loladze, I. Hidden shift of the ionome of plants exposed to elevated CO(2)depletes
411 minerals at the base of human nutrition. *Elife* **3**, e02245 (2014).
412 https://doi.org:10.7554/eLife.02245

413 3 Bouain, N. *et al.* Plant growth stimulation by high CO2 depends on phosphorus
414 homeostasis in chloroplasts. *Curr Biol* (2022).
415 https://doi.org:10.1016/j.cub.2022.08.032

416 4 Cassan, O. *et al.* A gene regulatory network in Arabidopsis roots reveals features and
417 regulators of the plant response to elevated CO(2). *New Phytol* (2023).
418 https://doi.org:10.1111/nph.18788

419 5 Sun, P. *et al.* Countering elevated CO2 induced Fe and Zn reduction in Arabidopsis
420 seeds. *New Phytol* **235**, 1796-1806 (2022). https://doi.org:10.1111/nph.18290

421 6 Umnajkitikorn, K., Sade, N., Rubio Wilhelmi, M. D. M., Gilbert, M. E. & Blumwald, E.
422 Silencing of OsCV (chloroplast vesiculation) maintained photorespiration and N
423 assimilation in rice plants grown under elevated CO(2). *Plant Cell Environ* **43**, 920-933
424 (2020). https://doi.org:10.1111/pce.13723

425 7 Yang, A., Li, Q., Chen, L. & Zhang, W.-H. A rice small GTPase, Rab6a, is involved in the
426 regulation of grain yield and iron nutrition in response to CO2 enrichment. *Journal of*
427 *Experimental Botany* **71**, 5680-5688 (2020). https://doi.org:10.1093/jxb/eraa279

428 8 Marcos-Barbero, E. L., Pérez, P., Martínez-Carrasco, R., Arellano, J. B. & Morcuende, R.
429 Screening for Higher Grain Yield and Biomass among Sixty Bread Wheat Genotypes
430 Grown under Elevated CO2 and High-Temperature Conditions. *Plants* **10**, 1596 (2021).
431 9 Myers, S. S. *et al.* Increasing CO2 threatens human nutrition. *Nature* **510**, 139-142
432 (2014). https://doi.org:10.1038/nature13179
433 10 Zhu, C. *et al.* Carbon dioxide (CO2) levels this century will alter the protein,
434 micronutrients, and vitamin content of rice grains with potential health consequences
435 for the poorest rice-dependent countries. *Sci Adv* **4**, eaaq1012 (2018).
436 https://doi.org:10.1126/sciadv.aaq1012
437 11 Arouisse, B., Korte, A., van Eeuwijk, F. & Kruijer, W. Imputation of 3 million SNPs in the
438 Arabidopsis regional mapping population. *The Plant Journal* **102**, 872-882 (2020).
439 https://doi.org:https://doi.org/10.1111/tpj.14659
440 12 Baxter, I. *et al.* A Coastal Cline in Sodium Accumulation in Arabidopsis thaliana Is Driven
441 by Natural Variation of the Sodium Transporter AtHKT1;1. *PLOS Genetics* **6**, e1001193
442 (2010). https://doi.org:10.1371/journal.pgen.1001193
443 13 North, K. A., Ehlting, B., Koprivova, A., Rennenberg, H. & Kopriva, S. Natural variation
444 in Arabidopsis adaptation to growth at low nitrogen conditions. *Plant Physiology and*
445 *Biochemistry* **47**, 912-918 (2009).
446 https://doi.org:https://doi.org/10.1016/j.plaphy.2009.06.009
447 14 Kim, S. *et al.* Recombination and linkage disequilibrium in Arabidopsis thaliana. *Nature*
448 *Genetics* **39**, 1151-1155 (2007). https://doi.org:10.1038/ng2115
449 15 Katz, E. *et al.* Genetic variation underlying differential ammonium and nitrate
450 responses in Arabidopsis thaliana. *The Plant Cell* **34**, 4696-4713 (2022).
451 https://doi.org:10.1093/plcell/koac279

452 16 Wang, Y. *et al.* AtTIP2;2 facilitates resistance to zinc toxicity via promoting zinc
453 immobilization in the root and limiting root-to-shoot zinc translocation in Arabidopsis
454 thaliana. *Ecotoxicology and Environmental Safety* **233**, 113333 (2022).
455 https://doi.org:https://doi.org/10.1016/j.ecoenv.2022.113333
456 17 Gaufichon, L. *et al.* ASN1-encoded asparagine synthetase in floral organs contributes
457 to nitrogen filling in Arabidopsis seeds. *The Plant Journal* **91**, 371-393 (2017).
458 https://doi.org:https://doi.org/10.1111/tpj.13567
459 18 Lam, H.-M. *et al.* Overexpression of the ASN1 Gene Enhances Nitrogen Status in Seeds
460 of Arabidopsis. *Plant Physiology* **132**, 926-935 (2003).
461 https://doi.org:10.1104/pp.103.020123
462 19 Li, Y. *et al.* Combined analyses of translatome and transcriptome in Arabidopsis reveal
463 new players responding to magnesium deficiency. *Journal of integrative plant biology*
464 **63**, 2075-2092 (2021). https://doi.org:https://doi.org/10.1111/jipb.13169
465 20 Brun, A. *et al.* MCO1 and MCO3, two putative ascorbate oxidases with ferroxidase
466 activity, new candidates for the regulation of apoplastic iron excess in Arabidopsis.
467 *Plant Direct* **6**, e463 (2022). https://doi.org:10.1002/pld3.463
468 21 Balk, J. & Schaedler, T. A. Iron cofactor assembly in plants. *Annu Rev Plant Biol* **65**, 125-
469 153 (2014). https://doi.org:10.1146/annurev-arplant-050213-035759
470 22 Ainsworth, E. A. & Long, S. P. What have we learned from 15 years of free-air CO2
471 enrichment (FACE)? A meta-analytic review of the responses of photosynthesis,
472 canopy properties and plant production to rising CO2. *New Phytol* **165**, 351-371 (2005).
473 https://doi.org:10.1111/j.1469-8137.2004.01224.x

23 Dusenge, M. E., Duarte, A. G. & Way, D. A. Plant carbon metabolism and climate change: elevated CO2 and temperature impacts on photosynthesis, photorespiration and respiration. *New Phytol* **221**, 32-49 (2019). https://doi.org:10.1111/nph.15283

24 Tausz-Posch, S., Tausz, M. & Bourgault, M. Elevated [CO2] effects on crops: Advances in understanding acclimation, nitrogen dynamics and interactions with drought and other organisms. *Plant Biol (Stuttg)* **22 Suppl 1**, 38-51 (2020). https://doi.org:10.1111/plb.12994

25 Thompson, M., Gamage, D., Hirotsu, N., Martin, A. & Seneweera, S. Effects of Elevated Carbon Dioxide on Photosynthesis and Carbon Partitioning: A Perspective on Root Sugar Sensing and Hormonal Crosstalk. *Front Physiol* **8**, 578 (2017). https://doi.org:10.3389/fphys.2017.00578

26 Luthi, D. *et al.* High-resolution carbon dioxide concentration record 650,000-800,000 years before present. *Nature* **453**, 379-382 (2008). https://doi.org:10.1038/nature06949

27 Pearson, P. N. & Palmer, M. R. Atmospheric carbon dioxide concentrations over the past 60 million years. *Nature* **406**, 695-699 (2000). https://doi.org:10.1038/35021000

28 Cortés, A. J. & López-Hernández, F. Harnessing Crop Wild Diversity for Climate Change Adaptation. *Genes* **12**, 783 (2021).

29 Pauls, S. U., Nowak, C., Balint, M. & Pfenninger, M. The impact of global climate change on genetic diversity within populations and species. *Mol Ecol* **22**, 925-946 (2013). https://doi.org:10.1111/mec.12152

30 Bohner, A., Kojima, S., Hajirezaei, M., Melzer, M. & von Wirén, N. Urea retranslocation from senescing Arabidopsis leaves is promoted by DUR3-mediated urea retrieval from

497 leaf apoplast. *The Plant Journal* **81**, 377-387 (2015).
498 https://doi.org:https://doi.org/10.1111/tpj.12740
499 31 Bloom, A. J., Burger, M., Rubio Asensio, J. S. & Cousins, A. B. Carbon dioxide enrichment
500 inhibits nitrate assimilation in wheat and Arabidopsis. *Science* **328**, 899-903 (2010).
501 https://doi.org:10.1126/science.1186440
502 32 Hu, H. *et al.* Distinct Cellular Locations of Carbonic Anhydrases Mediate Carbon Dioxide
503 Control of Stomatal Movements *Plant Physiology* **169**, 1168-1178 (2015).
504 https://doi.org:10.1104/pp.15.00646
505 33 Sharma, N. *et al.* Arabidopsis stromal carbonic anhydrases exhibit non-overlapping
506 roles in photosynthetic efficiency and development. *Plant J* **n/a** (2023).
507 https://doi.org:10.1111/tpj.16231
508 34 Shahzad, Z. & Rouached, H. Protecting plant nutrition from the effects of climate
509 change. *Curr Biol* **32**, R725-R727 (2022). https://doi.org:10.1016/j.cub.2022.05.056
510 35 Gansel, X., Munos, S., Tillard, P. & Gojon, A. Differential regulation of the NO3- and
511 NH4+ transporter genes AtNrt2.1 and AtAmt1.1 in Arabidopsis: relation with long-
512 distance and local controls by N status of the plant. *Plant J* **26**, 143-155 (2001).
513 36 Cassan, O., Lebre, S. & Martin, A. Inferring and analyzing gene regulatory networks
514 from multi-factorial expression data: a complete and interactive suite. *BMC Genomics*
515 **22**, 387 (2021). https://doi.org:10.1186/s12864-021-07659-2
516

Figure legends :

Figure 1: Elevated CO_2 negatively impacts the ionome content at the population-scale level in *Arabidopsis thaliana*. A. Representation of the experimental design used in this study. The content of eight mineral elements was assessed for around 600 *Arabidopsis thaliana* accessions coming from the REGMAP (B), LANGUEDOC (C) and TOU-A (D) populations. Each dot represents the value of the content of a mineral element for one accession (yellow: ambient CO_2 (aCO_2, ~420 ppm), blue: elevated CO_2 (eCO_2, 900 ppm). N (% of dry weight), Fe ($\mu g.g^{-1}$ dry weight), Zn ($\mu g.g^{-1}$ dry weight), Cu ($\mu g.g^{-1}$ dry weight), Mg ($\mu g.g^{-1}$ dry weight), Mn ($\mu g.g^{-1}$ dry weight), Na ($\mu g.g^{-1}$ dry weight), C (% of dry weight). Asterisks indicate significant differences (Paired Wilcoxson test; *, $P < 0.05$; **, $P < 0.005$; ***, $P < 0.0005$). ns; not significant.

Figure 2: Elevated CO_2 leads to high phenotypic diversity of ionome response in *Arabidopsis thaliana.* Distributions of the relative change (%) of the content of 8 mineral elements between elevated CO_2 and ambient CO_2, in each population (A: REGMAP, B: LANGUEDOC, C: TOU-A). Each dot represents the value of the relative change of the content a mineral element for one accession. The name of the element appears in bold if the mean of the element in elevated CO_2 is significantly different from the mean of the element in ambient CO_2 (Paired wilcoxon test, significance threshold of 0.05).

Figure 3: Elevated CO_2 results in a general pattern of ionome variation common to most accessions constituting natural populations of *Arabidopsis thaliana.* Principal Component Analysis (PCA) was performed using the variation of each element in response to elevated CO_2.

A. Natural accessions were positioned on the PCA and colored based on population. B. Contribution of each element to the PCA axis.

Figure 4: Variation in the response of the ionome to elevated CO_2 identifies contrasting subpopulations inside the REGMAP panel. K-means clustering was performed in the REGMAP accessions to identify different subpopulations. Each accession is represented by a dot, connected by a line between each element. Cluster 1:65 accessions. Cluster 2: 25 accessions. Cluster 3: 69 accessions.

Figure 5: Genetic architecture of the response of the ionome to elevated CO_2 in the REGMAP panel of *Arabidopsis thaliana.* A. Manhattan plots for the content of eight mineral elements under elevated CO_2, or for the relative change of the content of mineral elements between elevated CO_2 and ambient CO_2. For each Manhattan plot, SNPs with the 50 most significant P-value, located above the horizontal line, are colored. Bar plots showing the number of SNPs identified by GWAs for traits under elevated CO_2 (B) or for the relative change of the content of mineral elements between elevated CO_2 and ambient CO_2 (C) that are unique to one element or shared between 2 or 3 traits.

Figure 6: Identification of genes detected by GWA mapping and differentially regulated by elevated CO_2. Intersection between elevated CO_2-DEG in shoot (A) or root (B) and genes identified by GWA mapping. UpSet plots display the number of elevated CO_2-DEG that are associated to a locus identified for the content or the relative change of one or several mineral elements under elevated CO_2. Illustration of the pattern of elevated CO_2-DEG in shoot (C) or root (D) also identified by GWA mapping.

Figure 7: Natural variation of the *TIP2;2* gene is associated with improved responses of Zn content to elevated CO_2. Manhattan plot of the relative change of Zn content between elevated CO2 and ambient CO2 showing the presence of a peak closed to the *TIP2;2* locus. B. Comparison of haplotypes and their relative change of Zn content between elevated CO_2 and ambient CO_2. Three SNPs located at the *TIP2;2* locus are associated to an improvement of Zn content under elevated CO_2 for accessions that possess them (haplotype 1) compared to the rest of the population (haplotype 0). C. Relative expression of *TIP2;2* in the roots under elevated CO_2 for accessions belonging to haplotype 0 or haplotype 1. Relative expression levels were calculated based on *UBQ10* as internal control. Horizontal black line represented the median of each group of haplotypes. ***P < 0,001, unpaired Mann-Whitney test. D. Shoot Zn content under elevated CO_2 for WT (Columbia) and *tip2;2-1* mutant belonging to haplotype 0 or haplotype 1. Data are presented as the mean (with SD) of 5 and 6 biological repeats for the WT and *tip2;2-1*, respectively. *P < 0.05, unpaired Mann-Whitney test.